

# Zeolite SSZ-53: An Extra-Large-Pore Zeolite with Interesting Catalytic Properties\*\*

Supak Tontisirin and Stefan Ernst\*

Dedicated to Süd-Chemie on the occasion of its 150th anniversary

Zeolites have found widespread use as catalysts in petroleum refining and petrochemistry and as selective adsorbents in separation and purification. A special class of zeolites comprises high-silica zeolites with extra-large pores (the term “extra-large” encompasses zeolites with pore openings delimited by rings with more than 12 tetrahedral ( $\text{SiO}_4$  or  $\text{AlO}_4$ ) centers)). Although such materials possess considerable potential in catalysis (and adsorption) with larger molecules, their catalytic potential has only scarcely been explored so far. One of the more recently discovered extra-large-pore zeolites is SSZ-53, which was discovered in the Chevron laboratories.<sup>[1,2]</sup> Its pore system consists of linear, non-interconnected channels with pore openings formed from elliptical 14-rings with an approximate size of  $0.65 \times 0.85 \text{ nm}^2$ .<sup>[3]</sup> The framework topology of SSZ-53 has been assigned the three letter code SFH by the Structure Commission of the International Zeolite Association.<sup>[4]</sup> Herein, we report on the hydrothermal synthesis of zeolite SSZ-53 and on its catalytic properties in the acid-catalyzed disproportionation of ethylbenzene and the conversion of *n*-decane on a bifunctional form of the zeolite.

The X-ray powder pattern of the as-synthesized B-SSZ-53, its calcined form, and the acid form of Al-SSZ-53 are depicted in Figure 1. From a comparison with published data,<sup>[1–3]</sup> it can be deduced that the as-synthesized sample of B-SSZ-53 is of good crystallinity and does not contain amorphous or crystalline impurities. The modification steps applied to the as-synthesized B-SSZ-53 apparently do not alter the structural integrity of the material.

The typical crystallite size and morphology of SSZ-53 can be seen from the scanning electron micrograph shown in Figure 2. The needlelike crystallites are around 1 to 2  $\mu\text{m}$  long, and there are no indications for the presence of amorphous materials or other crystalline phases in the sample. Chemical analysis reveals that the Al-containing form of SSZ-53 prepared in the present study has a  $n_{\text{Si}}/n_{\text{Al}}$  ratio of 55:1. Moreover,  $\text{N}_2$  adsorption at 77 K (BET measurement) yields a specific surface area of about

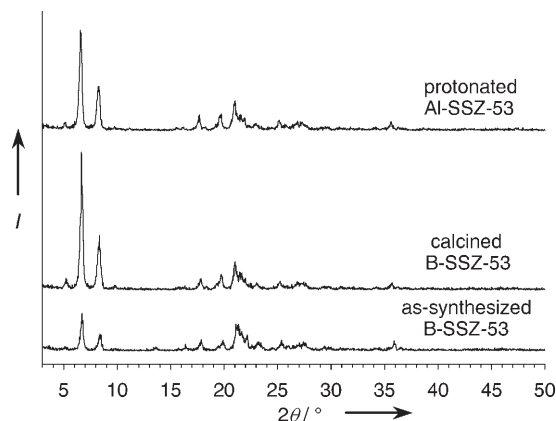


Figure 1. X-ray powder patterns of B-SSZ-53 in its as-synthesized and calcined form and of protonated Al-SSZ-53 (HSSZ-53).

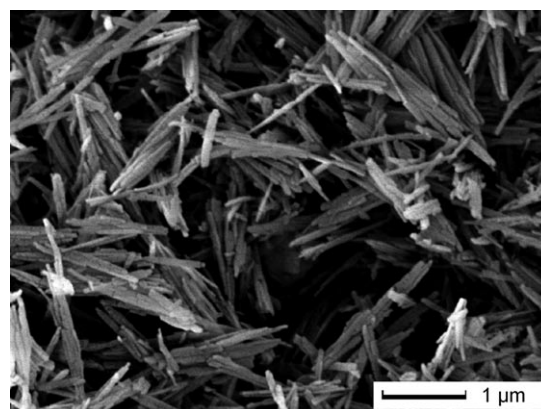


Figure 2. Scanning electron micrograph of calcined B-SSZ-53.

$440 \text{ m}^2 \text{ g}^{-1}$  and a specific pore volume of about  $0.19 \text{ cm}^3 \text{ g}^{-1}$ . These values are in good agreement with previously published data.<sup>[1–3]</sup>

The disproportionation of ethylbenzene to benzene and the three diethylbenzene isomers was first introduced by Karge et al. as a catalytic test reaction for the properties of acid zeolite catalysts.<sup>[5,6]</sup> Moreover, it has been demonstrated that this reaction can be exploited to distinguish between medium- and large-pore zeolites, based on the reaction selectivities.<sup>[7]</sup> More recently, the Catalysis Commission of the International Zeolites Association also has recommended the disproportionation of ethylbenzene as a test reaction for the characterization of acid zeolites.<sup>[8]</sup> The results with HSSZ-53 as the catalyst in the disproportionation of ethylbenzene are depicted in Figure 3. Already at a reaction temperature as

[\*] M.Sc. S. Tontisirin, Prof. Dr.-Ing. S. Ernst  
Fachbereich Chemie, Technische Chemie  
Technische Universität Kaiserslautern  
Erwin-Schroedinger-Strasse 54, 67663 Kaiserslautern (Germany)  
Fax: (+49) 631-205-4193  
E-mail: ernst@chemie.uni-kl.de

[\*\*] Financial support of this work by the Stiftung Rheinland-Pfalz für Innovation, Paul und Yvonne Gillet-Stiftung, and Fonds der Chemischen Industrie is gratefully acknowledged.

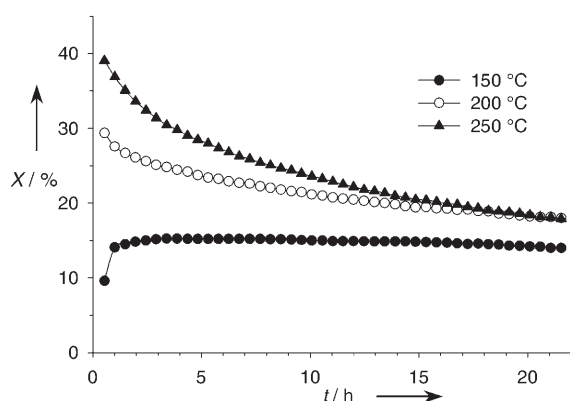


**Figure 3.** Disproportionation of ethylbenzene over HSSZ-53 at different temperatures ( $W_{\text{cat}}/F_{\text{EB}} = 290 \text{ g h mol}^{-1}$ ;  $W_{\text{cat}} = 290 \text{ mg}$ ).

low as 150 °C, conversions around 15 % are achieved. In addition, an induction period is initially observed (i.e. during the first two hours) during which the conversion increases and then levels-off into a quasi-stationary stage. All this is typical for large-pore zeolites.<sup>[5–7]</sup> With increasing reaction temperatures, ethylbenzene conversion increases; however, the induction period shortens or disappears completely (in agreement with literature reports).<sup>[7,8]</sup> Moreover, catalyst deactivation, that is, a decrease of conversion with time-on-stream, is observed with increasing reaction temperature. This is most probably due to coke formation as a result of undesired side reactions.

Figure 4 shows the conversion of ethylbenzene and the observed product yields at a reaction temperature of 200 °C as a function of time-on-stream. Ideally, pure ethylbenzene disproportionation should result in the formation of equal molar amounts of benzene and diethylbenzenes. It has, however, repeatedly been observed with large-pore zeolites that the molar ratio of diethylbenzenes to benzene is not strictly 1:1. Rather, a small diethylbenzene deficit is found, resulting in diethylbenzene/benzene ratios around 0.9:1.<sup>[7,8]</sup> This discrepancy (viz. the “loss” of ethylene groups) has been attributed to the formation of higher alkylated aromatics that are strongly adsorbed on the zeolite and/or to consecutive disproportionation of diethylbenzenes (DEB) with ethyl-

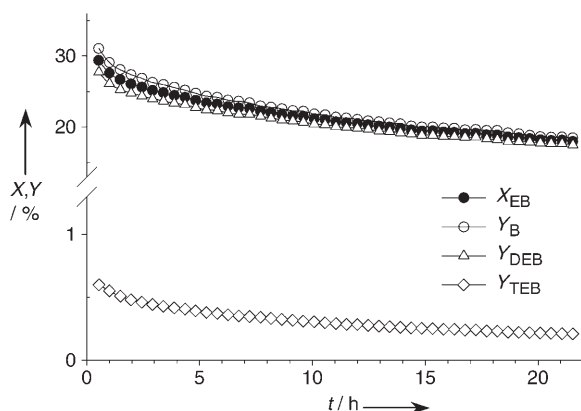


**Figure 4.** Conversion and product yields in the disproportionation of ethylbenzene over HSSZ-53 ( $T_{\text{R}} = 200 \text{ °C}$ ,  $W_{\text{cat}}/F_{\text{EB}} = 290 \text{ g h mol}^{-1}$ ,  $W_{\text{cat}} = 290 \text{ mg}$ ).

benzene to triethylbenzenes (TEB) and benzene. Indeed, triethylbenzenes were found in small amounts and at relatively high conversions over zeolite HSSZ-53 as catalyst (cf. Figure 4). Moreover, also a slow deactivation is observed, which is tentatively attributed to the formation of carbon-rich residues on the catalyst (“coke”).

The catalytic properties of the bifunctional form of SSZ-53 (0.27 Pd/HSSZ-53; Pd content: 0.27 wt %) were explored in the isomerization and hydrocracking of *n*-decane. This reaction has been frequently used for probing the effective pore width of zeolite catalysts.<sup>[9,10]</sup> The conversion of *n*-decane and the yields of isomers and hydrocracked products as a function of the reaction temperature are depicted in Figure 5. It can be seen that conversion starts already at about 170 °C and is virtually complete at 300 °C.

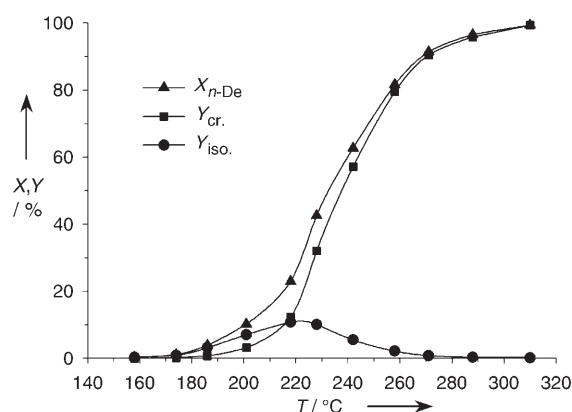


**Figure 5.** Influence of the reaction temperature on the conversion of *n*-decane (*n*-De), as well as on the yields of the isomers and hydrocracked products over 0.27 Pd/HSSZ-53 as catalyst ( $p_{\text{H}_2} \approx 101.3 \text{ kPa}$ ;  $n_{\text{H}_2}/n_{n\text{-De}} \approx 100$ ;  $W_{\text{cat}}/F_{n\text{-De}} = 400 \text{ g h mol}^{-1}$ ).

As usually observed, skeletal isomerization of linear *n*-decane to branched isoalkanes is the sole reaction at very low conversions. Moreover, monobranched isomers appear initially in the product and are, with increasing conversion, converted to dibranched isomers. Among the monobranched species, the different (2-, 3-, 4-, and 5-) methylnonanes predominate with selectivities around 70 to 80 %. The selectivity ratio of 2- and 5-methylnonane formed at low conversion is about 1.7:1 and is therefore typical for very-large-pore zeolites.<sup>[9,10]</sup> The remaining monobranched isomers consist of 3- and 4-ethyloctane (20 to 30 %) and minor amounts of 4-propylheptane (up to ca. 1 %). All this is again typical for very-large-pore zeolites.<sup>[9,10]</sup> Moreover, the formation of these large amounts of monobranched isomers with side chains longer than methyl groups could be of advantage in, for example, dewaxing by isomerization, leading to improved cold flow properties of the dewaxed oil.

Hydrocracking already starts at low conversions and consumes the branched  $\text{C}_{10}$  isomers (Figure 5). The generally low yield of isomers together with an unsymmetrical distribution of the hydrocracked products (Figure 6), is typical for zeolites with one-dimensional pores (e.g., mordenite) and has been rationalized with a hindered diffusion of  $\text{C}_{10}$  moieties in the unidimensional channels, leading to enhanced hydro-

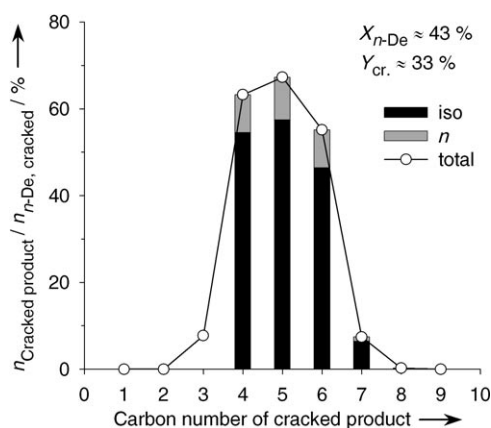


**Figure 6.** Distribution of cracked products from *n*-decane over 0.27 Pd/HSSZ-53 at  $X_{n-De} \approx 43\%$  and  $Y_{cr} \approx 33\%$ .

cracking.<sup>[10,11]</sup> With increasing conversion, hydrocracking starts and consumes the branched  $C_{10}$  isomers. A typical distribution of the hydrocracked products is shown in Figure 6. It can be seen that  $C_1$  and  $C_2$  as well as  $C_8$  and  $C_9$  hydrocarbons are absent. This suggests that hydrogenolysis, namely hydrocracking at the noble metal, is absent and the predominating reaction mechanism is really a bifunctional one.<sup>[12]</sup> From the slightly asymmetric shape of the distribution of the hydrocracked products, it can be deduced that some minor contribution of secondary cracking occurs. Moreover, branched isomers predominate in the  $C_4$  to  $C_7$  fractions, which indicates that hydrocracking starts from highly branched intermediates. This reflects the large space available in the channels of the extra-large-pore zeolite SSZ-53. In particular, the molar amount of isopentane formed from 100 moles of hydrocracked *n*-decane (at ca. 35% yield of cracked products) has been shown to be a valuable measure for the space available around the catalytic sites. A value of 58 is found for zeolite SSZ-53 which is comparable to values of about 54 for Y-type zeolites with their large intracrystalline supercages of about 1.3 nm in diameter.<sup>[10,11]</sup>

In conclusion, it has been shown that zeolite SSZ-53 is a highly active extra-large-pore zeolite. The results of the test reactions for probing its effective pore width under catalytically relevant conditions are in agreement with its crystallographic structure. Due to its high hydrocracking activity and its large effective pore size, SSZ-53 seems to be particularly suitable for the hydrocracking of more bulky molecules. This makes it an attractive candidate for applications in petroleum refining.

## Experimental Section

Zeolite SSZ-53 was initially synthesized as borosilicate (B-SSZ-53) and then converted to the catalytically more active and more stable aluminosilicate form by post-synthetic treatments. B-SSZ-53 was synthesized according to a modified procedure derived from the literature.<sup>[1,2]</sup> The structure-directing agent required for the synthesis step (*N,N,N*-trimethyl-1-[1-(4-fluorophenyl)cyclopentyl]methylammonium hydroxide) was prepared as described previously.<sup>[1]</sup> In a typical synthesis, an aqueous solution of the template (concentration:  $0.965 \text{ mol kg}^{-1}$ ) was diluted with distilled water (15 g) and then

added to a mixture of NaOH (0.047 g) and sodium borate decahydrate (0.1 g). The resulting mixture was stirred until the solid dissolved. Subsequently, Cab-O-Sil M5 (1.5 g, 97 wt %  $\text{SiO}_2$ , 3 wt % water) were slowly added and the resulting gel stirred for another 0.5 h. The gel was then transferred to a 25-mL stainless-steel autoclave with a Teflon-liner. Crystallization was achieved in the rotating autoclave (40 revolutions per min) at  $160^\circ\text{C}$  over seven days. The obtained crystalline solid was washed with distilled water and then heated ( $1.5^\circ\text{C min}^{-1}$ ) to  $540^\circ\text{C}$  in a flow of  $\text{N}_2$ . Then the gas flow was switched to air and the temperature was kept constant for 5 h. The sample was then heated to  $594^\circ\text{C}$  and kept there for 5 h. From the calcined B-SSZ-53, acidic Al-SSZ-53 was obtained by ion-exchanging the calcined form for 12 h at  $95^\circ\text{C}$  in an excess of a 1N aluminum nitrate solution, followed by filtration and washing the resulting solid with distilled water. After drying at  $100^\circ\text{C}$  for 12 h and a final calcination at  $540^\circ\text{C}$  in a flow of  $\text{N}_2$ , the acid (H-) form of Al-SSZ-53 (HSSZ-53) was obtained. The bifunctional form of this material was prepared by ion-exchange with an appropriate amount of an aqueous solution of  $[\text{Pd}(\text{NH}_3)_4]\text{Cl}_2$  such as to obtain a final palladium loading of 0.27 wt %. Prior to the catalytic experiments on the disproportionation of ethylbenzene, the H-form of the catalyst was calcined in situ in the reactor at  $400^\circ\text{C}$  in  $\text{N}_2$  for 12 h. For the bifunctional conversion of *n*-decane, the Pd-loaded catalyst was calcined at  $400^\circ\text{C}$  in  $\text{N}_2$  for 12 h, at  $300^\circ\text{C}$  in air for 7 h, and then reduced at  $300^\circ\text{C}$  in  $\text{H}_2$  for 10 h. The catalytic experiments were conducted under atmospheric pressure in a fixed-bed flow-type apparatus with on-line analysis using temperature-programmed capillary gas chromatography. For the disproportionation of ethylbenzene,  $\text{N}_2$  was used as carrier gas with a partial pressure of the feed  $p_{EB}$  of 1 kPa. For the bifunctional conversion of *n*-decane, hydrogen was used as carrier gas and the partial pressure of *n*-decane amounted to 1 kPa.

Received: April 13, 2007

Revised: June 1, 2007

Published online: September 6, 2007

**Keywords:** heterogeneous catalysis · microporous materials · SSZ-53 · zeolites

- [1] S. Elomari (Chevron Research and Technology Company), WO-A1 01/9992155, **2001**.
- [2] S. A. Elomari, S. I. Zones in *Studies in Surface Science and Catalysis, Vol. 135* (Eds.: A. Galarneau, F. Di Renzo, F. Fajula, J. Vedrine), Elsevier, Amsterdam, **2001**, pp. 479–486.
- [3] A. Burton, S. Elomari, C.-Y. Chen, R. C. Medrud, I. Y. Chan, L. M. Bull, C. Kibby, T. V. Harris, S. I. Zones, E. S. Vittoratos, *Chem. Eur. J.* **2003**, *9*, 5737–5748.
- [4] <http://www.iza-online.org/databases/>.
- [5] H. G. Karge, J. Ladebeck, Z. Sarbak, K. Hatada, *Zeolites* **1982**, *2*, 94–102.
- [6] H. G. Karge, K. Hatada, Y. Zhang, R. Fiedorow, *Zeolites* **1983**, *3*, 13–21.
- [7] J. Weitkamp, S. Ernst, P. A. Jacobs, H. G. Karge, *Erdoel Kohle Erdgas Petrochem.* **1986**, *39*, 13–18.
- [8] D. E. De Vos, S. Ernst, C. Perego, C. T. O'Connor, M. Stöcker, *Microporous Mesoporous Mater.* **2002**, *56*, 185–192.
- [9] J. A. Martens, M. Tielen, P. A. Jacobs, J. Weitkamp, *Zeolites* **1984**, *4*, 98–107.
- [10] J. A. Martens, P. A. Jacobs, *Zeolites* **1986**, *6*, 334–348.
- [11] M. M. Olken, J. M. Garces in *Proceedings from the Ninth International Zeolite Conference, Vol. II* (Eds.: R. von Ballmoos, J. B. Higgins, M. M. J. Treacy), Butterworth-Heinemann, Stoneham, **1993**, pp. 559–566.
- [12] J. Weitkamp, S. Ernst in *Guidelines for Mastering the Properties of Molecular Sieves* (Eds.: D. Barthomeuf, E. G. Derouane, W. Hölderich), Plenum, New York, **1990**, pp. 343–353.